Energy Technology
Generation, Conversion, Storage, Distribution
www.entechnol.de

Organic Amines as Targeting Stabilizer at the Polymer/Fullerene Interface for Polymer:$PC_{61}BM$ Solar Cells

*Zerui Li, Lingpeng Yan, Jiankai Shan, Huimin Gu, Yi Lin, Yaling Wang, Hongwei Tan, and Chang-Qi Ma**

Herein, it is demonstrated that a small amount (0.05% in weight ratio) of polyethyleneimine (PEI) can effectively suppress the "burn-in" degradation of both PTB7-Th:$PC_{61}BM$ and P3HT:$PC_{61}BM$ cells, similar to the piperazine derivatives, suggesting that organic amines can serve as universal stabilizer in polymer:$PC_{61}BM$ solar cells. Light-induced electron spin resonance (LESR) spectroscopy measurement shows a higher ESR signal intensity of $PC_{61}BM$ anions in 0.2% PEI-doped film than in 1% piperazine-doped film. Moreover, no piperazine is detected in a 10% (w/w) piperazine-doped film by gas chromatography–mass spectrometry (GS—MS). These results suggest that the residual piperazine in the blend film is very low, which can be understood by the high volatility of piperazine. Quantum calculations are performed on the intermolecular binding energy (E_B) between polymer (using model repeating units), $PC_{61}BM$, and piperazine molecules. Results reveal that piperazine prefers to localize at the polymer:fullerene interface by complexing with $PC_{61}BM$ (in P3HT:$PC_{61}BM$) or PTB7-Th (in PTB7-Th:$PC_{61}BM$ system), which indicates that the photo dimerization of $PC_{61}BM$ which causes the "burn-in" degradation of polymer:fullerene solar cells mainly happens at the donor/acceptor interface, and the organic amine serves as the targeting stabilizer at the interface.

1. Introduction

Polymer solar cell (PSC) has been considered as one of the most promising photovoltaic technologies because of its variety of advantages, including potential low cost,[1] excellent flexibility,[2] light weight,[3] and ease of large-area fabrication.[4] With over 30 years' development, the power conversion efficiency (PCE) of PSCs has recently achieved a highest record of over 18%,[5] making PSCs close to the commercial application. However, the relatively low stability of PSC is still an impediment to commercialization, and lengthening the lifetime is becoming the next most important topic for PSCs.[6] It has been reported that most of the PSCs suffer a "burn-in" degradation, which leads to a fast performance decay (about 30–50% PCE loss) at the first hundred hours.[7] For polymer:fullerene solar cells, the dimerization of fullerene is considered as the main reason for the fast "burn-in" degradation of the device performance.[8] Our recent work demonstrated that such a fast performance decay can be suppressed by doping the photoactive layer with piperazine, which is attributed to the photo-induced intermolecular charge transfer between piperazine and $PC_{61}BM$ that suppresses the following dimerization process of fullerene molecules.[9] In our investigation on the molecular structure depended stabilization effect of the piperazine derivatives (PZs), it is found that only the N—H containing PZs show effective stabilization effect, which comes from the intermolecular hydrogen bonds between N—H of PZs and $PC_{61}BM$.[10] The intermolecular hydrogen bonds bring piperazine molecule close enough to $PC_{61}BM$ to form steady adduct, which would promote the photo-induced electron transfer between these two components and suppress the fullerene dimerization, thus improving the stability of solar cells.[10] Furthermore, piperazine doping is also applicable in PTB7-Th:$PC_{61}BM$ and PffBT4T-2OD:$PC_{61}BM$ solar cell system, showing the broad spectrum of piperazine in stabilizing the performance of PSCs.[9] These findings remind us

Z. Li, Prof. C.-Q. Ma
School of Nano-Tech and Nano-Bionics
University of Science and Technology of China
398 Jinzhai Road, Hefei 230026, P. R. China
E-mail: cqma2011@sinano.ac.cn

Z. Li, Dr. L. Yan, H. Gu, Dr. Y. Wang, Prof. C.-Q. Ma
Printable Electronics Research Center
Suzhou Institute of Nano-Tech and Nano-Bionics
Chinese Academy of Sciences
Ruoshui Road 398, SEID, SIP, Suzhou 215123, P. R. China

The ORCID identification number(s) for the author(s) of this article can be found under https://doi.org/10.1002/ente.202000266.

DOI: 10.1002/ente.202000266

Dr. L. Yan
Institute of New Carbon Materials
Taiyuan University of Technology
79 Yingze Street, Taiyuan 030024, P. R. China

J. Shan, Prof. H. Tan
College of Chemistry
Beijing Normal University, Beijing
19 Waida Street, Xinjie Kou, Beijing 100875, P. R. China

Dr. Y. Lin
Department of Chemistry
Xi'an Jiaotong Liverpool University
Renai Road 11, SEDI, SIP, Suzhou 215123, P. R. China

that organic amine could be an effective stabilizer for polymer:$PC_{61}BM$ solar cells as well. Interestingly, coumarin derivatives were also found to be able to improve the performance and stability of PSCs, both in fullerene and nonfullerene solar cell systems, which was attributed to the formation of intermolecular hydrogen bonding between coumarin and $PC_{71}BM$ or ITIC through N—H...O=C bonds.[11] In addition, H...π bond between polarized N—H groups and electron-rich π-conjugation systems (e.g., C_{60}) is a kind of hydrogen bond that exists in many molecule systems.[12] It can be expected that organic amines which contain N—H bond should be able to complex with $PC_{61}BM$ through intermolecular hydrogen bonds. Polyethyleneimine (PEI) has primary and secondary amine units within the molecule. Although it has been widely used as the interfacial layer to modify solar cells,[13] there isn't any report yet about adding PEI into active layer to improve the performance and stability of PSCs. In this article, for the first time, we demonstrated that PEI could also serve as an effective stabilizer in polymer:fullerene solar cells. However, the optimal doping concentration is much lower than piperazine in P3HT:$PC_{61}BM$. By investigating the residual concentration of piperazine and the interaction between piperazine and polymer or $PC_{61}BM$, we demonstrate that organic amine molecules mostly locate at the donor–acceptor interface. These results also confirmed that the dimerization of $PC_{61}BM$ that causes the "burn-in" degradation of polymer:$PC_{61}BM$ solar cells mainly happens at the donor–acceptor interface and organic amine is a kind of targeting stabilizer for polymer:$PC_{61}BM$ solar cells.

2. Results and Discussion

2.1. PEI Doping Effect on the Performance and Stability of the Cells

The device structure and the molecular structure of the chemicals are shown in **Figure 1**. PEI molecule has both primary and secondary amine groups, which is a good model compound of organic amine for the stabilization effect study. Also, PEI is a nonvolatile molecule and this enables us to compare the influence of molecular size and volatility of the organic amine on the stabilization effect. First, the doping effect of PEI on the performance and stability of the PTB7-Th:$PC_{61}BM$ cells were investigated. As PEI is insoluble in chlorobenzene (CB), PEI was first dissolved in ethanol, and the PEI ethanol solution was mixed with PTB7-Th:$PC_{61}BM$ (in CB) for the preparation of the photoactive layer. The blend ratio of ethanol and CB is 1:9. To exclude the effect of ethanol on the performance and stability, the reference PEI-free PTB7-Th:$PC_{61}BM$ cells were also prepared from the same mixture solvent.

The representative *J–V* curves and external quantum efficiency (EQE) spectra of the PTB7-Th:$PC_{61}BM$:PEI cells are shown in **Figure 2**a,b, and the performance data are listed in **Table 1**. As seen here, the averaged PCE of reference PTB7-Th:$PC_{61}BM$ cells is 8.27%, which is comparable to the values reported in the literature,[14] suggesting the ignorable negative effect of ethanol mixing in solar-cell fabrication. When PEI doping concentration is lower than 0.05%, slightly increased performance was measured for the doped cells (8.39% and 8.33% for 0.01% and 0.05% cells, respectively). Further increase in PEI doping concentration to 0.10%, however, decreases the device performance to lower than 8% (Table 1). Nevertheless, the photovoltaic performance results indicated that these PTB7-Th:$PC_{61}BM$ cells were well optimized, and they are suitable for the following stability comparison.

The photovoltaic devices were then aged in the glovebox under continuous light illumination, and the performance decay curves of these cells are shown in **Figure 3**. For the reference devices, the time reaches 80% of its initial PCE (T_{80}) was determined to be 2 h (due to the fast decay in fill factor [FF]), and only 59% of its initial PCE remained after aging for 300 h (η_{300}/η_0), demonstrating clear "burn-in" degradation process. It can be seen here that the devices with 0.01% PEI showed similar degradation process

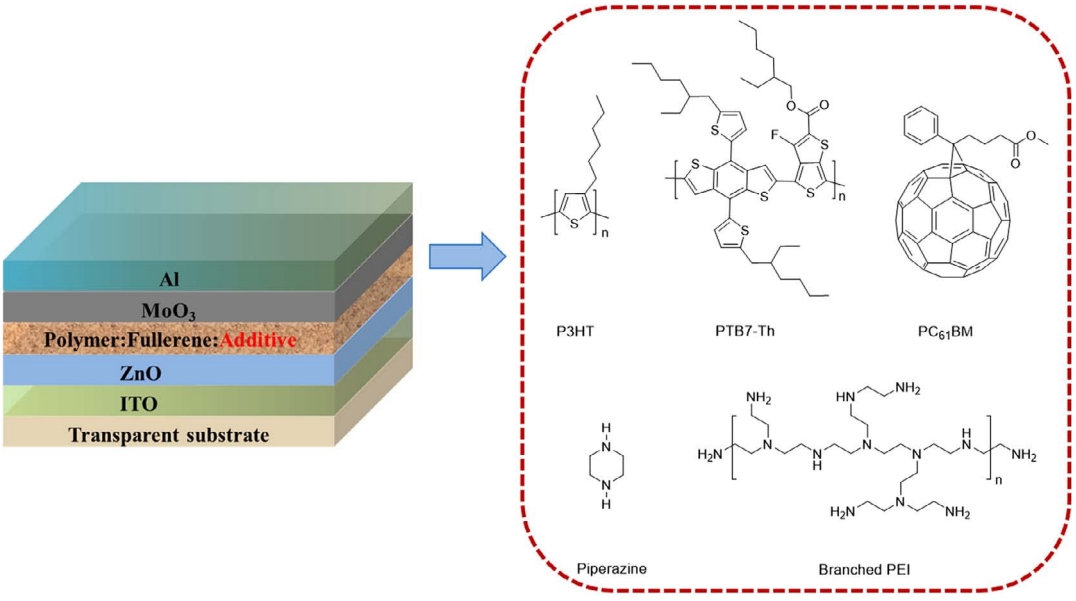

Figure 1. Structure of the PSCs as well as the molecular structures of materials used in this study.

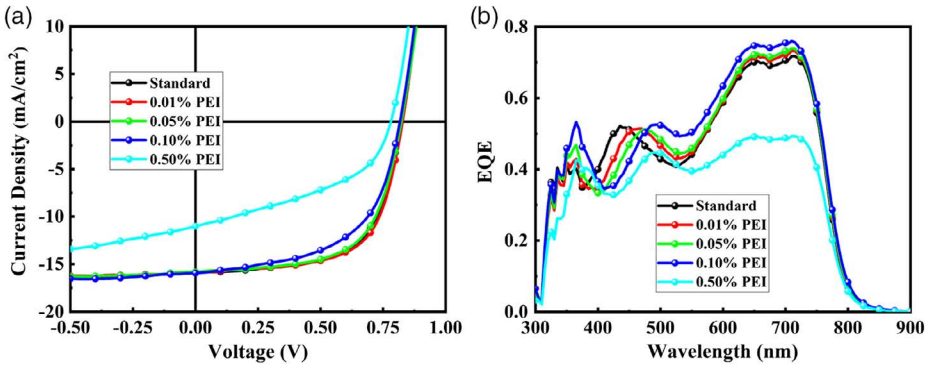

Figure 2. a) *J–V* curves and b) EQE spectra of PTB7-Th:$PC_{61}BM$ cells doped with PEI.

Table 1. Photovoltaic performance of the PTB7-Th:$PC_{61}BM$ and P3HT:$PC_{61}BM$ cells with different PEI doping concentration.

	PEI doping concentration [%]	V_{OC} [V]	J_{SC} [mA cm^{-2}]	FF	PCE [%]	T_{80} [h][a)]	η_{300}/η_0 [%][b)]
PTB7-Th:$PC_{61}BM$	None	0.823 ± 0.001	15.95 ± 0.09	0.63 ± 0.00	8.27 ± 0.06	2	59
	0.01	0.828 ± 0.003	15.78 ± 0.15	0.64 ± 0.00	8.39 ± 0.08	2	66
	0.05	0.824 ± 0.001	15.90 ± 0.06	0.64 ± 0.00	8.33 ± 0.08	82	70
	0.10	0.818 ± 0.001	16.02 ± 0.16	0.55 ± 0.01	7.23 ± 0.15	139	72
	0.50	0.781 ± 0.001	10.78 ± 0.41	0.43 ± 0.00	3.60 ± 0.12	231	77
P3HT:$PC_{61}BM$	None	0.587 ± 0.007	10.18 ± 0.23	0.54 ± 0.01	3.21 ± 0.09	17	65
	0.05	0.577 ± 0.001	9.31 ± 0.18	0.56 ± 0.01	3.03 ± 0.05	≫300[c)]	104
	0.10	0.576 ± 0.001	9.47 ± 0.02	0.55 ± 0.01	3.02 ± 0.11	≫300[c)]	102
	0.20	0.562 ± 0.002	8.54 ± 0.18	0.57 ± 0.00	2.71 ± 0.05	≫300[c)]	97
	0.30	0.560 ± 0.002	7.96 ± 0.17	0.57 ± 0.00	2.55 ± 0.07	≫300[c)]	100

[a)]Time that reach the 80% of its initial PCE; [b)]η_0: PCE of the cell before aging, η_{300}: PCE of the cell after aging for 300 h; [c)]As the measuring time was limited to 300 h, the performance did not reach the 80% of the initial PCE.

as reference devices, of which the T_{80} is almost the same as reference ones (2 h, due to the fast decay in FF as well), and the η_{300} raises slightly to 66%, suggesting too little PEI hardly had stabilization effect. However, when the doping concentration of PEI increased gradually to 0.05% and 0.10%, the doped devices showed much better stability, where the T_{80} got longer (82 h and 139 h, respectively) and the relative PCE got higher (η_{300}/η_0 equals 70% and 72%, respectively). To be specific, such a stability improvement mainly reflects in J_{SC}, which is similar to piperazine and demonstrates the stabilization effect from PEI on fullerene dimerization. For the higher concentration doping condition, such as 0.50%, although the device performance decreased greatly, an obvious improvement in illumination stability was also observed (T_{80} ≈231 h, η_{300} ≈77%). For higher-concentration situations, the degradation of doping devices mainly comes from FF and obvious distinctions could be found in the degradation process of J_{SC}, indicating the excellent stabilization effect of PEI doping in PTB7-Th:$PC_{61}BM$.

To further verify the doping effect of PEI in polymer:fullerene solar cells, P3HT:$PC_{61}BM$ cells doped with PEI were also fabricated and tested. Note that both the reference cell and the PEI-doped cells were made from the ethanol:*ortho*-dichlorobenzene mixture solvent with a blending ratio of 1:9. **Figure 4**a,b show the representative *J–V* curves and EQE spectra of the P3HT:$PC_{61}BM$ solar cells doping with PEI, and the performance data are listed in Table 1. As seen here, the averaged PCE of reference P3HT:$PC_{61}BM$ cells is 3.2%, which is comparable to the results reported in the literature.[15] When the PEI doping concentration is relatively low (less than 0.1%), the doped cells showed slightly lower PCE than the reference cells. Similar to the PTB7-Th:$PC_{61}BM$ cells, device performance decreases dramatically with the increase in PEI doping concentration, where a low PCE of 2.5% was obtained with 0.3% PEI doping. Also, the cells with PCE around 3% are comparable for the stability study.

All these cells were then aged inside the glovebox with continuous light illumination. **Figure 5** shows the performance decay curves of these cells. As seen here, the pristine P3HT:$PC_{61}BM$ cells showed fast "burn-in" performance decay at the first hundred hours, similar to our previous report,[8c,9–10] suggesting that ethanol mixing in the solvent does not increase the stability of the cells. The time reaches 80% of its initial PCE (T_{80}) was determined to be 17 h, and only 65% of its initial PCE remained after aging for 300 h (η_{300}). In contrast, the PEI-doped cells showed great stability improvement (η_{300}/η_0 ≈100%) after aging for 300 h, clearly demonstrating the same function of stabilization effect of PEI as piperazine in P3HT:$PC_{61}BM$.

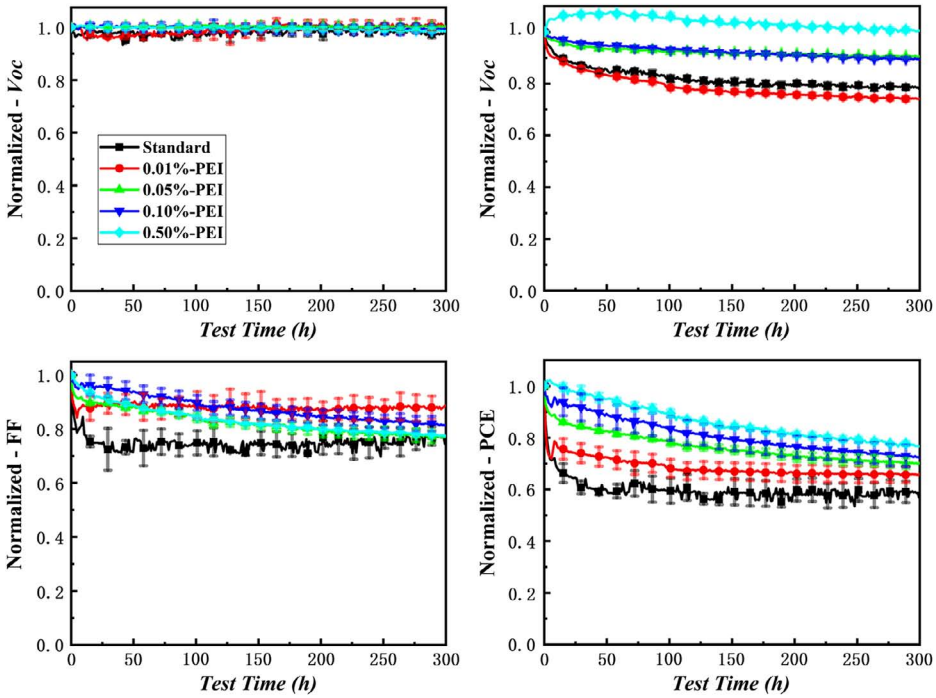

Figure 3. Degradation curves of PTB7-Th:$PC_{61}BM$ cells doped with PEI.

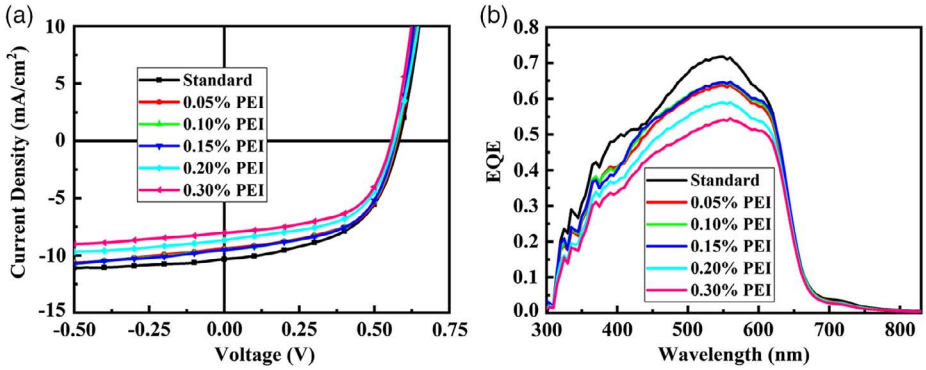

Figure 4. a) *J–V* curves and b) EQE spectra of P3HT:$PC_{61}BM$ cells doped with PEI.

Furthermore, the concentration of PEI is extremely low, as even 0.05% mass fraction of P3HT:$PC_{61}BM$ brings great improvement in the stabilization.

Although the optimal PEI doping concentration for the PTB7-Th:$PC_{61}BM$ and P3HT:$PC_{61}BM$ cells are slightly different in respect to the device performance, doping the photoactive layer with PEI can stabilize the device performance, clearly demonstrating the stabilization effect of PEI molecules. Along with the effective stabilization effect of N—H bond containing piperazine molecules,[10] we suppose that organic amines with N—H bonds should be able to serve as the stabilizer in polymer:fullerene solar cells, yet the optimal doping concentration need to be carefully optimized.

It could be seen earlier that too much PEI would cause an clear decrease in device performance. Similar results about the negative effect from amine group on PSC performance were found in amine-group modified active layer, which was attributed to be an ultrafast trapping process in active layer film that seriously cripples hole transport and results in very poor device performance.[16] The additive concentration in the current case is low as 0.1% PEI, which is much lower than that in those reports; we therefore suspect that such a poor performance comes from the changes in the nanomorphology of the active layer. Transmission electron microscopy (TEM) was then performed on the PTB7-Th:$PC_{61}BM$ films to investigate the effect of PEI doping on the morphology of the photoactive layer. **Figure 6** shows the TEM results. As seen here, the 0.01% PEI-doped PTB7-Th:$PC_{61}BM$ cells show a morphology with very fine nanofibers, which is similar to the reference film. However, when PEI doping concentration is higher than 0.1%, huge phase separation is detected, which is believed as the reason for the low device performance upon high PEI doping. Based on the understanding

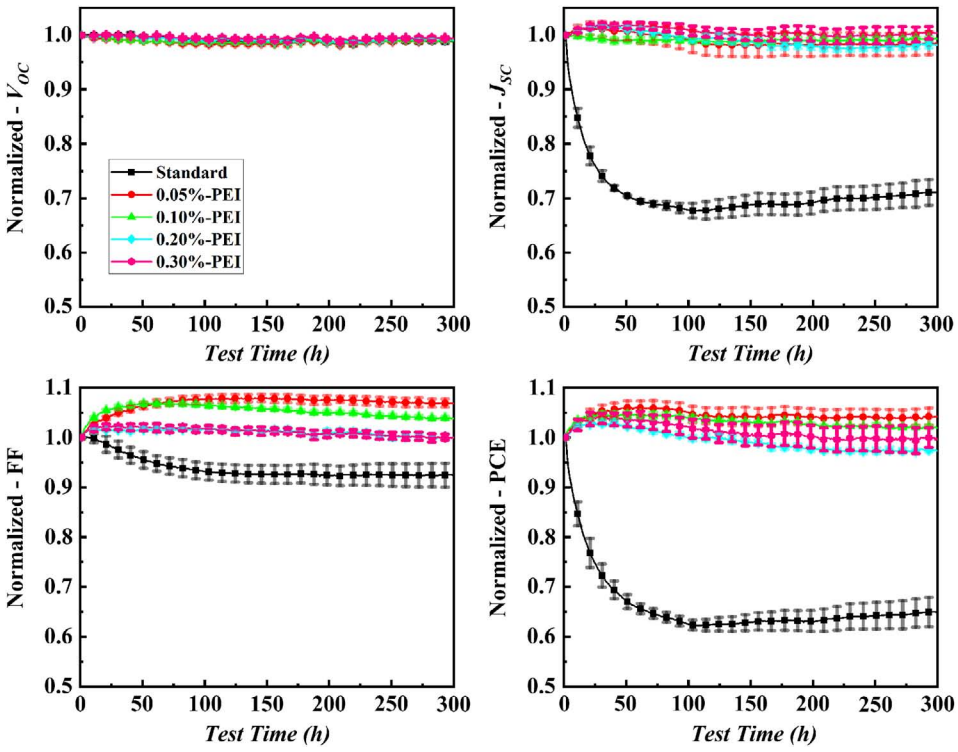

Figure 5. Degradation curves of P3HT:$PC_{61}BM$ cells doped with PEI.

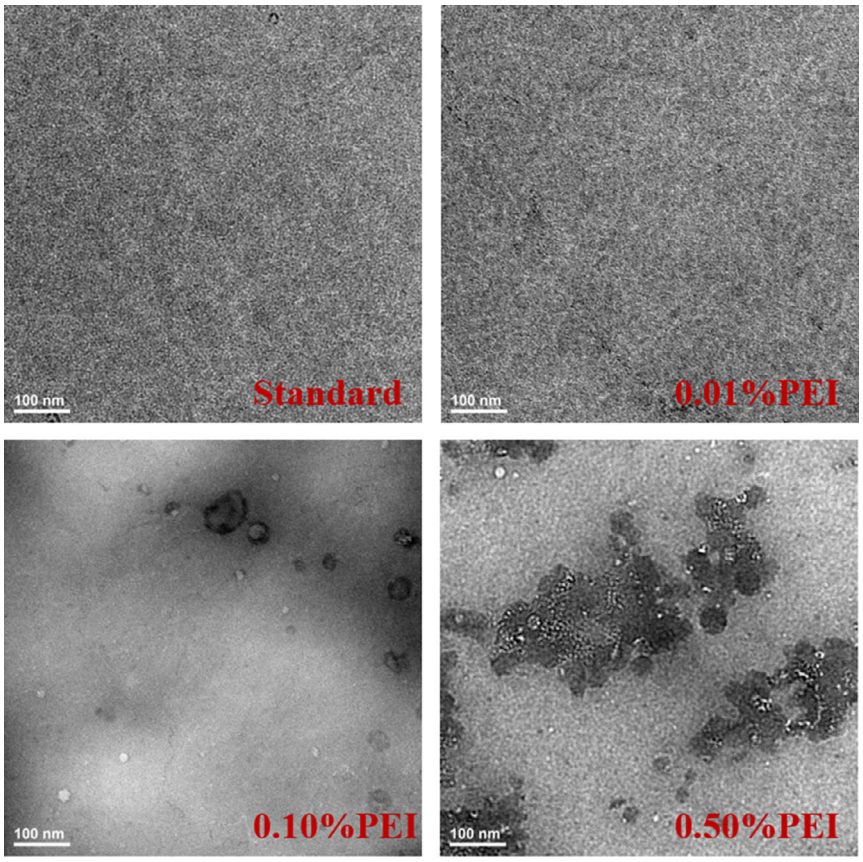

Figure 6. TEM images of PTB7-Th:$PC_{61}BM$ films doped with different PEI concentration (in weight ratio).

of stabilization mechanism of piperazine in polymer:fullerene solar cells,[9,10] we attribute the stabilization effect of PEI to the existence of N—H bonds and the electron-donating capability of PEI, rather than the improvement in nanomorphology.

2.2. Interaction of PEI and Piperazine with $PC_{61}BM$

Electron spin resonance (ESR) measurement is a powerful method for probing the creation of radical species in the polymer blend films,[17] which is related to the stability of PSCs. Our recent LESR measurements demonstrated that light-induced electron transfer between PZs and $PC_{61}BM$ happens, yielding $PC_{61}BM$ radical anion that is directly related to the stabilization effect of the PZs.[9,10] ESR of the $PC_{61}BM$, $PC_{61}BM$:piperazine and $PC_{61}BM$:PEI films were then measured at 90 K with or without light illumination. **Figure 7** shows the results. As seen here, no $PC_{61}BM$ anion signal (for the $PC_{61}BM$ and $PC_{61}BM$:piperazine films) or very weak $PC_{61}BM$ anion signal at $g = 1.9999$[18] (for $PC_{61}BM$:PEI films) was measured when these films are kept in the dark, indicating weak interaction between $PC_{61}BM$ and organic amine in the dark. When these samples were illuminated with light, except for the $PC_{61}BM$ net film, where no $PC_{61}BM$ anion signal was measured, the other two films showed clear $PC_{61}BM$ anion signals. Interestingly, the $PC_{61}BM$ anion signal intensity of the PEI-doped film is much higher than that of the piperazine-doped film, although the PEI doping concentration (0.2%) is only one-fifth of piperazine. As both amines have similar molecular structures, and the difference between the oxidation potential of amine and reduction potential of $PC_{61}BM$ is not the main driving force for the photo-induced electron transfer,[9,10] such an ESR signal intensity difference indicates the residual concentration of piperazine might be much lower than PEI, although the initial piperazine doping concentration is five times higher than PEI, which could be due to the high volatility of piperazine.

2.3. Low Piperazine Residual in the Final P3HT:$PC_{61}BM$ Blend Film

To understand the difference between piperazine and PEI in the stabilization effect, we then tried to analyze the residual piperazine in the final blend films quantitively. We used GC–MS to check the piperazine within the films (See Figure S1, Supporting Information). A "Signal intensity–Concentration" curve for the GC trace of the piperazine-blended P3HT:$PC_{61}BM$ solution was then established (see Figure S2, Supporting Information). With this, the detection limit of piperazine is determined to be 1.2 mg mL^{-1} in our experiment system. We then prepared the P3HT:$PC_{61}BM$:piperazine film by drop-casting mixture solution with a blend ratio of 20:20:4 mg mL^{-1}. The thin solid film was then dissolved again in chloroform in half volume of its initial number. If all piperazine molecules were "dissolved" in the P3HT:$PC_{61}BM$ film, the corresponding piperazine concentration should be 8 mg mL^{-1} in the solution sample for GC–MS measurement. However, no piperazine signal was detected for sample solution, indicating that the real piperazine concentration in P3HT:$PC_{61}BM$ thin film is less than 1.2 mg mL^{-1}. This result confirmed that over 70% piperazine evaporated during the preparation of thin solid film. It is not a big surprise as piperazine is volatile and it sublimates at a rather high heating temperature (see Figure S3, Supporting Information) and thermal annealing at 124 °C for 10 min as well as thermal evaporation in vacuum are necessary for the preparation of photoactive layer (see Experimental Section for details). This result explains well why the ESR signal in the $PC_{61}BM$:piperazine is much lower than that in $PC_{61}BM$:PEI. Furthermore, the low residual piperazine concentration within the blend film suggests that the stabilization effect of piperazine in polymer:fullerene solar cells might not be due to the stabilization of nanomorphology as supposed by Zhang et al.,[19] but more related to the quenching of fullerene excitons.

2.4. Distribution of Amine in the Active Layer and the Thin-Film Formation Mechanism

To further understand the interaction between organic amines and fullerene molecules, quantum chemical calculation was performed on P3HT:$PC_{61}BM$:piperazine and PTB7-Th:$PC_{61}BM$:piperazine systems with special focus on the binding energy between polymer, fullerene, and piperazine molecules. To simplify the calculation, we use regioregular hexi(3-hexylthiophene) 6T and oligomers BDT-TT (basic repeating unit of PTB7-Th) as the model of P3HT and PTB7-Th (See Figure S4, Supporting Information for the chemical structure of 6T and BDT-TT). **Figure 8** lists the calculated binding energy (E_B) for different molecule combinations. The E_B of two piperazine molecules

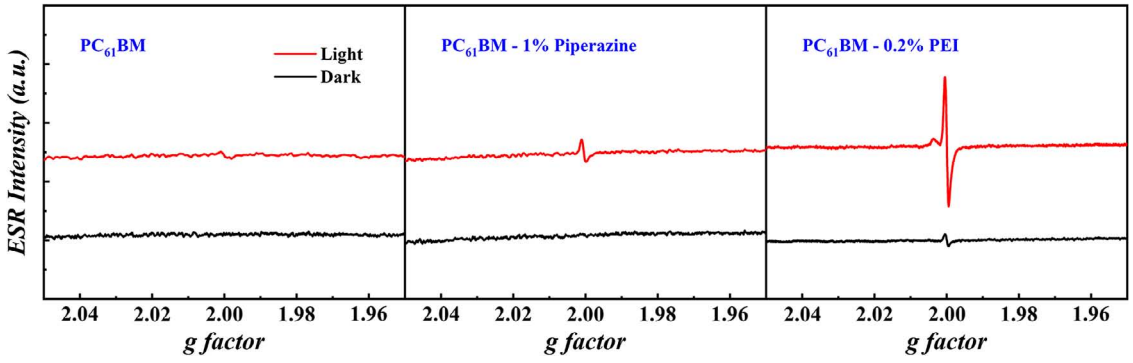

Figure 7. ESR spectra of $PC_{61}BM$-amine blend films measured at 90 K.

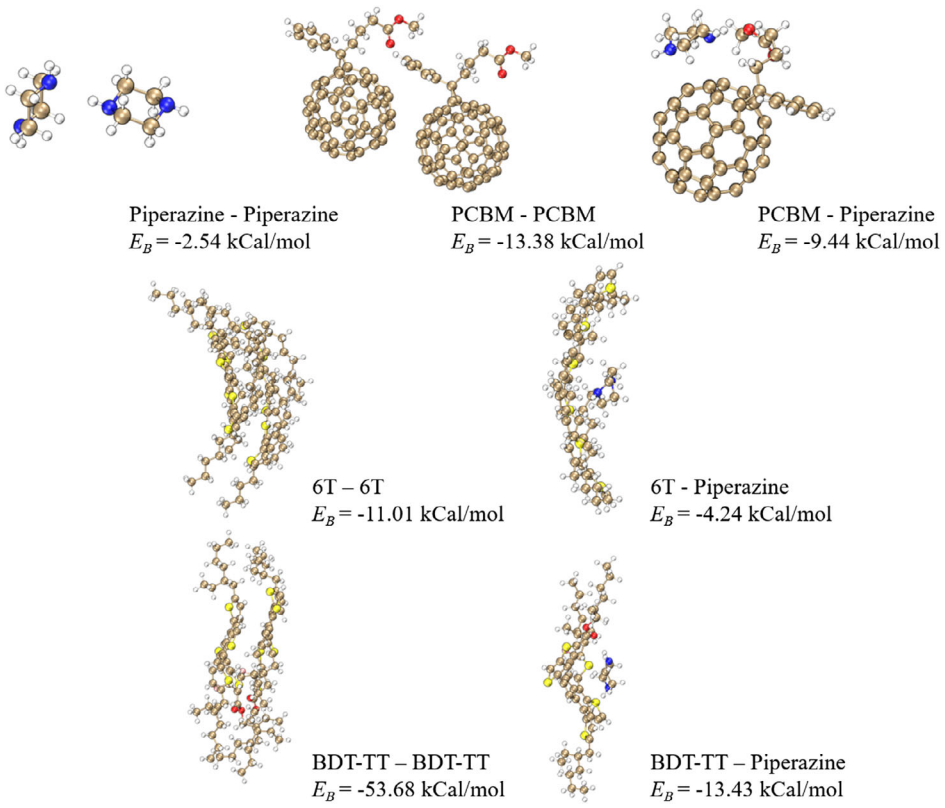

Figure 8. Calculated binding energy of different molecule combinations.

is calculated to be $-2.54\,\text{kcal mol}^{-1}$, indicating the weak intermolecular interaction between piperazine molecules, which is in good accordance with the volatility of piperazine. In P3HT:$PC_{61}BM$:piperazine blend, due to the existence of intermolecular H-bonding, the E_B of $PC_{61}BM$:piperazine ($-9.44\,\text{kCal mol}^{-1}$) is higher than that of 6T:piperazine ($-4.24\,\text{kCal mol}^{-1}$), indicating that piperazine is mostly complex with $PC_{61}BM$ in the P3HT:$PC_{61}BM$ blend. Meanwhile, the E_B of $PC_{61}BM$:piperazine is lower than 6T:6T ($-11.01\,\text{kCal mol}^{-1}$) and $PC_{61}BM$:$PC_{61}BM$ complex ($-13.38\,\text{kCal mol}^{-1}$), suggesting that it is rather difficult for the piperazine molecule to diffuse into the crystalline P3HT and $PC_{61}BM$ domains. In other words, piperazine molecules mostly localize on the interfaces of P3HT and $PC_{61}BM$ domains and complex with $PC_{61}BM$.

In BDB-T:TT:piperazine complex, the bond length of H···O between the N—H of piperazine and O=C of thienothiophene was calculated to be 2.13 Å, which is shorter than the sum of the van der Waals radii of H (1.08 Å) and O (1.40 Å),[20] suggesting the formation of H-bonding between these two molecules (Figure S5, Supporting Information). Due to the existence of H-bonding, the E_B of BDT-TT:piperazine was calculated to be $-13.43\,\text{kCal mol}^{-1}$, which is higher than that of $PC_{61}BM$:piperazine complex, suggesting that piperazine is most likely complex with PTB7-Th rather than $PC_{61}BM$ in the PTB7-Th:$PC_{61}BM$ blend film. Moreover, the E_B of BDT-TT:piperazine is much lower than that of BDT-TT:BDT-TT ($53.68\,\text{kCal mol}^{-1}$), suggesting that piperazine is also less likely to diffuse into the PTB7-Th crystalline domains in the blend film. Therefore, piperazine molecules also mostly localize at the PTB7-Th/$PC_{61}BM$ interfaces, as the P3HT:$PC_{61}BM$ blend film.

With these, a thin-film formation mechanism is proposed as in **Figure 9**. At the early stage of the spin coating, polymer, fullerene, and piperazine molecules are homogeneously dispersed in the solution (stage I). During the spin coating, polymer and fullerene molecules start homocrystallization under the driven force of the decrease in enthalpy, whereas piperazine molecules are dispersed in the amorphous polymer:fullerene matrix (stage II). In the last stage, large polymer and fullerene crystals form and piperazine molecules escape from the blend system due to the high volatility of piperazine, leaving a small amount of piperazine localized at the grain boundary of the donor–acceptor domains (stage III).

2.5. Further Discussion

It is worthy also to point out that our initial test prove that doping of organic amines (either piperazine or PEI) does not improve the performance and stability of polymer:nonfullerene acceptor (NFA) solar cells (not published results). This suggests that the NFA-based solar cells have different decay mechanism to the polymer:fullerene solar cells. Understanding the detailed degradation mechanism of polymer:NFA solar cells is still needed. Nevertheless, as described earlier, doping the polymer:fullerene photoactive layer with 0.1% of organic amine can already effectively suppress the fast "burn-in" degradation caused by the photo-induced dimerization of $PC_{61}BM$. In combination with

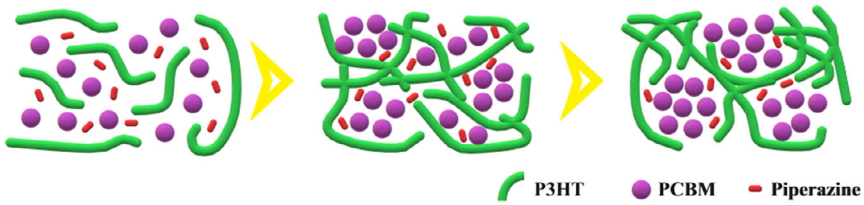

Figure 9. Proposed thin-film formation of polymer:fullerene:piperazine blend system.

the conclusion that organic amine molecules mostly localize at the donor–acceptor interface, one can conclude that photo dimerization of $PC_{61}BM$ mainly happens at the donor–acceptor interfaces. This also brings to a conclusion that polymer:$PC_{61}BM$ cells with larger crystalline domains should decay slower than those who have too small phase separation within the blend film, which is in good accordance with the findings of Brabec and co-workers, where thermal annealing the P3HT:$PC_{61}BM$ films slowed the J_{SC} decay of the cell due to the increased crystallinity of the fullerene domain.[19,21] In contrast, as organic amine stabilizer molecules mostly localize at the donor–acceptor interface, the optimal doping concentration of the stabilizer must be sensitive to the nanomorphology of the photoactive layer as well as the volatility of the stabilizer.

3. Conclusion

In conclusion, we proved that PEI is an alternative of piperazine in stabilizing the performance of polymer:fullerene solar cells, demonstrating that organic amine can serve as a universal stabilizer in polymer:fullerene solar cells. In contrast to piperazine, the optimal doping concentration of PEI in P3HT:$PC_{61}BM$ was found to be as low as 0.1%. However, higher ESR signal of $PC_{61}BM$ radical anion was measured in the PEI film (with 0.2% doping concentration) than in the piperazine-doped film (1%), although piperazine doping concentration is much higher than PEI. This result indicates that the residual piperazine doping concentration in the blend film is quite low, which is attributed to the high volatility of piperazine. Quantum chemical calculations on the intermolecular interactions between polymer, fullerene, and piperazine molecules confirmed that polymer and fullerene trend to homocrystallization, and piperazine molecules mainly localize at the donor–acceptor interface, which on the one hand explains why organic amine can effectively suppress the "burn-in" performance decay even at a very low doping concentration, and on the other hand, indicates the photo dimerization of $PC_{61}BM$ molecules happens at the donor–acceptor interface.

4. Experimental Section

Materials: ITO substrates are custom-made on glass with strip width of 3 mm. Regioregular poly(3-hexylthiophene-2,5-diyl) (P3HT, $M_w = 50\,000$, PDI = 2.0–2.4, regioregularity $R_r = 91$–94%) and poly[4,8-bis (5-(2-ethylhexyl)thiophen-2-yl)benzo[1,2-*b*;4,5-*b'*]dithiophene-2,6-diyl-alt-(4-(2-ethylhexyl)-3-fluorothieno[3,4-*b*]thiophene-)-2-carboxylate-2-6-diyl)] (PTB7-Th, $M_w = 40\,000$, PDI = 1.8–2.0) were purchased from Solarmer Energy, Inc. (Beijing). [6,6]-phenyl-C_{61}-butyric acid methyl ester ($PC_{61}BM$) was purchased from American Dye Source, Inc. (Canada). 1,8-Diiodooctane (DIO) was purchased from TCI (Shanghai). Piperazine was purchased from Adamas-Beta. PEI (average $M_n \approx 10\,000$ by GPC, branched) was purchased from Sigma Aldrich. Molybdenum (VI) oxide (MoO_3) was purchased from Strem Chemicals. Inc. All materials were used as received without further purification. ZnO nanoparticles solution was prepared through the reaction between KOH and $Zn(OAc)_2$ in methanol as reported by Beek et al.[22]

Instruments and Measurements: Light-induced electron spin resonance (LESR) test was carried out with an ESR spectrometer (Bruker E500). The sample was prepared by putting a solution of $PC_{61}BM$ or $PC_{61}BM$:amine in *ortho*-dichlorobenzene (ODCB) (200 µL, 20 mg mL^{-1} for $PC_{61}BM$) into a standard 5 mm nuclear magnetic resonance tube, and the solvent was removed under vacuum and a thin film was formed on the tube wall. The measurements were carried out at 90 K with or without light illumination from a xenon lamp (wavelength range from 200 to 800 nm). Gas chromatography–mass spectrometry (GC–MS) was performed with a GC–MS spectrometer (Agilent 7890A/5975C). The P3HT:$PC_{61}BM$ blend solution with piperazine (1–10%, corresponding to 0.4–4.0 mg mL^{-1} for piperazine) were taken to test for a "Signal intensity–Concentration" curve. Then P3HT:$PC_{61}BM$:piperazine (10% doping) film was prepared by drop-casting 0.5 mL solution onto a 5 × 5 cm^{2}glass substrate and then dried inside glovebox without thermal heating. After that, the thin solid film was washed with 1 mL chloroform, and then concentrated to 0.25 mL inside the fume hood. TEM images of active layers were obtained from a Tecnai G2 F20 S-Twin 200 kV field-emission electron microscope (FEI). The photoactive layers for TEM measurement were prepared by spin-coating the solution onto the UV-treated glass substrate, followed by a treatment of HF vapor in a fume hood.

Simulation and Quantum Chemistry Calculation: All theoretical calculations were carried out using the Gaussian 09 program.[23] All the species were optimized using the B3LYP density functional with the def2-svp basis set.[24] Dispersion corrections were accounted using an empirical formula by Grimme with Becke–Johnson damping.[25] Basis set superposition error corrections were considered in calculating the interaction energies.[26] The molecular radii of the molecules were estimated using Multiwfn.[27]

Fabrication of Organic Solar Cells: ITO substrates were sequentially cleaned by ultrasonic bath in detergent, deionized water, acetone, and isopropanol, and then were kept in isopropanol. The substrates were then treated in a UV–ozone oven for 30 min before used. First, filtered ZnO solution (12 mg mL^{-1} in methanol) was spin-coated on the ITO substrates at 3000 rpm for 60 s. Then, the samples were annealed at 130 °C for 10 min on a hot plate. The PTB7-Th:$PC_{61}BM$ (1.0:1.5 w/w, with a total concentration of 27.8 mg mL^{-1} in CB) and P3HT:$PC_{61}BM$ (1.0/1.0 w/w, with a total concentration of 44.4 mg mL^{-1} in ODCB) precursor solutions were prepared in advance. PEI solutions in ethanol with concentrations of 0.2, 1.0, and 2 mg mL^{-1} were then prepared. The final PTB7-Th:$PC_{61}BM$:PEI and P3HT:$PC_{61}BM$:PEI solutions were then prepared by mixing the corresponding precursor solution with piperazine ethanol solution (and a necessary amount of ethanol to fit the total CB or ODCB to ethanol ratio of 9:1 v/v, see detailed data in Table S1, Supporting Information). The solutions were stirred at 60 °C for 3 h (for the PTB7-Th:$PC_{61}BM$:PEI) or 55 °C overnight (for the P3HT:$PC_{61}BM$:PEI solution) before use. DIO (3% in volume ratio) was used in the PTB7-Th:$PC_{61}BM$:PEI system. The polymer:fullerene:PEI films were prepared by spin-coating the solution on ZnO films with 2000 rpm for 60 s (for the PTB7-Th:$PC_{61}BM$:PEI) or 600 rpm

for 60 s (for the P3HT:$PC_{61}BM$:PEI). The as-prepared PTB7-Th:$PC_{61}BM$:PEI blend films were then put into vacuum for 1 h to remove the DIO, whereas the P3HT:$PC_{61}BM$:PEI films were solvent annealed in a Petri dish with ODCB for 1.5 h and then heated at 120 °C for 10 min. Finally, MoO_3 (20 nm) and Al (100 nm) were sequentially vacuum deposited on the top of the active layer as the hole-extraction layer and the anode, respectively. The effective photovoltaic area was 0.09 cm^2 which was defined by the geometrical overlap between the bottom cathode electrode and the top anode.

Performance Characterization of Organic Solar Cells: The performance of the devices was measured using a Keithley 2400 SourceMeter under illumination with simulated AM 1.5G sunlight (Verasol-2, LED 3A Sun simulator, Newport) in a nitrogen-filled glovebox. The *J–V* curves were recorded and then V_{OC}, J_{SC}, FF, and PCE were calculated through a home-programmed software. The EQE spectra were recorded under a simulated one sun operation condition using bias light from a 532 nm solid-state laser. A 150 W tungsten halogen lamp (Osram 64610) was used as the source for probe light, which was modulated with a mechanical chopper and selected the wavelength through a monochromator (Zolix, Omni-k300). The response was recorded as the voltage by a *J–V* converter (DNR-IV Convertor, Suzhou D&R Instruments) with a lock-in amplifier (Stanford Research Systems SR 830). Before testing devices, a calibrated silicon cell was used as the reference. The device for EQE measurement was kept in a nitrogen-filled container with a quartz window.

Degradation of Organic Solar Cells Performance under Illumination: The long-term stability of unencapsulated devices was conducted with a glovebox integrated multichannel solar cell performance decay test system (PVLT-G8001M, Suzhou D&R Instruments Co. Ltd.) under a testing condition in accordance with ISOS-L-1. The devices were put inside a nitrogen-filled glovebox ($H_2O < 1$ ppm, $O_2 < 1$ ppm) and continuously illuminated with white light-emitting diode (LED) light (D&R Light, L-W5300KA-150, Suzhou D&R Instruments). The illumination light intensity was initially set before testing to make sure the output short-circuit current density (J_{SC}) equals the value that measured under standard conditions mentioned earlier. The illumination light intensity was monitored by a photodiode (Hamamtsu S1336-8BQ) to guarantee stable light intensity. *J–V* characters of the devices were checked periodically, and the photovoltaic performance data (V_{OC}, J_{SC}, FF, and PCE) were calculated automatically according to the *J–V* curves. After *J–V* sweeping, an external load that match the maximum power output point ($R_{mpp} = V_{max}/I_{max}$) was attached to the cells so that the devices work at their maximum power point. The performance data of devices under illumination were recorded automatically over time and the degradation curves were shown. As external load was changed according to the *J–V* results, the measured performance decay curves could imply the performance decay behavior of cells under real operation, which fully met the load requirement for the highest level of ISOS-L3. The cell temperature was measured occasionally, and the temperature range during aging was about 45–55 °C.

Supporting Information

Supporting Information is available from the Wiley Online Library or from the author.

Acknowledgements

The authors would like to acknowledge the financial support from the Ministry of Science and Technology of China (No. 2016YFA0200700), the National Natural Science Foundation of China (21571019, 61904121), Chinese Academy of Science (No. YJKYYQ20180029, and CAS-ITRI 2019010).

Conflict of Interest

The authors declare no conflict of interest.

Keywords

organic amines, polymer solar cells, quantum calculations, stabilizers

Received: March 23, 2020
Revised: April 20, 2020
Published online:

[1] C. K. Sun, F. Pan, H. J. Bin, J. Q. Zhang, L. W. Xue, B. B. Qiu, Z. X. Wei, Z. G. Zhang, Y. F. Li, *Nat. Commun.* **2018**, *9*, 743.
[2] a) Y. Han, X. Chen, J. Wei, G. Ji, C. Wang, W. Zhao, J. Lai, W. Zha, Z. Li, L. Yan, *Adv. Sci.* *6*, **2019**, 1901490; b) H. Jinno, K. Fukuda, X. M. Xu, S. Park, Y. Suzuki, M. Koizumi, T. Yokota, I. Osaka, K. Takimiya, T. Someya, *Nat. Energy* **2017**, *2*, 780.
[3] M. Kaltenbrunner, M. S. White, E. D. Glowacki, T. Sekitani, T. Someya, N. S. Sariciftci, S. Bauer, *Nat. Commun.* **2012**, *3*, 770.
[4] S. Dong, K. Zhang, B. M. Xie, J. Y. Xiao, H. L. Yip, H. Yan, F. Huang, Y. Cao, *Adv. Energy Mater.* **2019**, *9*, 1802832.
[5] Q. Liu, Y. Jiang, K. Jin, J. Qin, J. Xu, W. Li, J. Xiong, J. Liu, Z. Xiao, K. Sun, *Sci. Bull.* **2020**, *65*, 272.
[6] a) W. R. Mateker, M. D. McGehee, *Adv. Mater.* **2017**, *29*, 1603940; b) R. M. Xue, J. W. Zhang, Y. W. Li, Y. F. Li, *Small* **2018**, *14*, 1801793.
[7] N. Li, J. D. Perea, T. Kassar, M. Richter, T. Heumueller, G. J. Matt, Y. Hou, N. S. Güldal, H. Chen, S. Chen, *Nat. Commun.* **2017**, *8*, 1.
[8] a) A. Distler, T. Sauermann, H. J. Egelhaaf, S. Rodman, D. Waller, K. S. Cheon, M. Lee, D. M. Guldi, *Adv. Energy Mater.* **2014**, *4*, 1300693; b) T. Heumueller, W. R. Mateker, A. Distler, U. F. Fritze, R. Cheacharoen, W. H. Nguyen, M. Biele, M. Salvador, M. von Delius, H.-J. Egelhaaf, M. D. McGehee, C. J. Brabec, *Energ. Environ. Sci.* **2016**, *9*, 247; c) L. P. Yan, J. D. Yi, Q. Chen, J. Y. Dou, Y. Z. Yang, X. G. Liu, L. W. Chen, C. Q. Ma, *J. Mater. Chem. A* **2017**, *5*, 10010.
[9] L. P. Yan, Y. L. Wang, J. F. Wei, G. Q. Ji, H. M. Gu, Z. R. Li, J. Q. Zhang, Q. Luo, Z. Q. Wang, X. G. Liu, B. S. Xu, Z. X. Wei, C. Q. Ma, *J. Mater. Chem. A* **2019**, *7*, 7099.
[10] Z. Li, J. Shan, L. Yan, H. Gu, Y. Lin, H. Tan, C.-Q. Ma, *ACS Appl. Mater. Interfaces* **2020**, *12*, 15472.
[11] a) X. Du, S. Tao, L. Li, W. Wang, C. Zheng, H. Lin, X. Zhang, X. Zhang, *Sol RRL* **2018**, *2*, 1800038; b) X. Kong, H. Lin, X. Du, L. Li, X. Li, X. Chen, C. Zheng, D. Wang, S. Tao, *J. Mater. Chem. C* **2018**, *6*, 9691.
[12] a) M. Keiluweit, M. Kleber, *Environ. Sci. Technol.* **2009**, *43*, 3421; b) N. Mohan, K. P. Vijayalakshmi, N. Koga, C. H. Suresh, *J. Comput. Chem.* **2010**, *31*, 2874.
[13] a) Y. Li, X. Qi, G. Liu, Y. Zhang, N. Zhu, Q. Zhang, X. Guo, D. Wang, H. Hu, Z. Chen, *Org. Electron* **2019**, *65*, 19; b) J. Wei, C. Zhang, G. Ji, Y. Han, I. Ismail, H. Li, Q. Luo, J. Yang, C.-Q. Ma, *Sol. Energy* **2019**, *193*, 102.
[14] a) C. H. Zhang, S. Langner, A. V. Mumyatov, D. V. Anokhin, J. Min, J. D. Perea, K. L. Gerasimov, A. Osvet, D. A. Ivanov, P. Troshin, N. Li, C. J. Brabec, *J. Mater. Chem. A* **2017**, *5*, 17570; b) C. H. Zhang, A. Mumyatov, S. Langner, J. D. Perea, T. Kassar, J. Min, L. L. Ke, H. W. Chen, K. L. Gerasimov, D. V. Anokhin, D. A. Ivanov, T. Ameri, A. Osvet, D. K. Susarova, T. Unruh, N. Li, P. Troshin, C. J. Brabec, *Adv. Energy Mater.* **2017**, *7*, 1601204.
[15] a) D. A. Chen, A. Nakahara, D. G. Wei, D. Nordlund, T. P. Russell, *Nano Lett.* **2011**, *11*, 561; b) M. T. Dang, L. Hirsch, G. Wantz, *Adv. Mater.* **2011**, *23*, 3597; c) D. M. Gonzalez, V. Korstgens, Y. Yao, L. Song, G. Santoro, S. V. Roth, P. Muller-Buschbaum, *Adv. Energy Mater.* **2015**, *5*, 1401770.
[16] a) C. H. Duan, W. Z. Cai, B. B. Y. Hsu, C. M. Zhong, K. Zhang, C. C. Liu, Z. C. Hu, F. Huang, G. C. Bazan, A. J. Heeger, Y. Cao,

Energ. Environ. Sci. **2013**, *6*, 3022; b) W. Z. Cai, C. M. Zhong, C. H. Duan, Z. C. Hu, S. Dong, D. R. Cao, M. Lei, F. Huang, Y. Cao, *Appl. Phys. Lett.* **2015**, *106*, 233302.

[17] a) L. A. Frolova, N. P. Piven, D. K. Susarova, A. V. Akkuratov, S. D. Babenko, P. A. Troshin, *Chem. Commun.* **2015**, *51*, 2242; b) D. K. Susarova, N. P. Piven, A. V. Akkuratov, L. A. Frolova, M. S. Polinskaya, S. A. Ponomarenko, S. D. Babenko, P. A. Troshin, *Chem. Commun.* **2015**, *51*, 2239; c) L. N. Inasaridze, A. I. Shames, I. V. Martynov, B. Li, A. V. Mumyatov, D. K. Susarova, E. A. Katz, P. A. Troshin, *J. Mater. Chem. A* **2017**, *5*, 8044.

[18] a) A. Aguirre, S. C. J. Meskers, R. A. J. Janssen, H. J. Egelhaaf, *Org. Electron* **2011**, *12*, 1657; b) M. Havlicek, N. S. Sariciftci, M. C. Scharber, *J. Mater. Res.* **2018**, *33*, 1853.

[19] C. H. Zhang, T. Heumueller, S. Leon, W. Gruber, K. Burlafinger, X. F. Tang, J. D. Perea, I. Wabra, A. Hirsch, T. Unruh, N. Li, C. J. Brabec, *Energ. Environ. Sci.* **2019**, *12*, 1078.

[20] S. Z. Hu, Z. H. Zhou, K. R. Tsai, *Acta Phys.-Chim. Sin.* **2003**, *19*, 1073.

[21] T. M. Grant, T. Gorisse, O. Dautel, G. Wantz, B. H. Lessard, *J. Mater. Chem. A* **2017**, *5*, 1581.

[22] W. J. E. Beek, M. M. Wienk, M. Kemerink, X. N. Yang, R. A. J. Janssen, *J. Phys. Chem. B* **2005**, *109*, 9505.

[23] M. J. Frisch, G. W. Trucks, H. B. Schlegel, G. E. Scuseria, M. A. Robb, J. R. Cheeseman, G. Scalmani, V. Barone, G. A. Petersson, H. Nakatsuji, X. Li, M. Caricato, A. V. Marenich, J. Bloino, B. G. Janesko, R. Gomperts, B. Mennucci, H. P. Hratchian, J. V. Ortiz, A. F. Izmaylov, J. L. Sonnenberg, W. F. Ding, F. Lipparini, F. Egidi, J. Goings, B. Peng, A. Petrone, T. Henderson, D. Ranasinghe, V. G. Zakrzewski, et al., *Gaussian* **2013**, *09*.

[24] a) P. J. Stephens, F. J. Devlin, C. F. Chabalowski, M. J. Frisch, *J. Phys. Chem.* **1994**, *98*, 11623; b) F. Weigend, R. Ahlrichs, *Phys. Chem. Chem. Phys.* **2005**, *7*, 3297.

[25] S. Grimme, S. Ehrlich, L. Goerigk, *J. Comput. Chem.* **2011**, *32*, 1456.

[26] a) S. Simon, M. Duran, J. J. Dannenberg, *J. Chem. Phys.* **1996**, *105*, 11024; b) S. F. Boys, F. Bernardi, *Mol. Phys.* **2002**, *100*, 65.

[27] T. Lu, F. W. Chen, *J. Comput. Chem.* **2012**, *33*, 580.